Available online at www.sciencedirect.com

ScienceDirect

Physics Procedia 81 (2016) 113 – 116

Physics Procedia

28th International Symposium on Superconductivity, ISS 2015, November 16-18, 2015, Tokyo, Japan

Microstructures of $YBa_2Cu_3O_y$ Layers Deposited on Conductive Layer-Buffered Metal Tapes

Ataru Ichinose[a,c,*], Masayuki Hashimoto[b], Shigeru Horii[b,c], Toshiya Doi[b,c]

[a]*Central Research Institute of Electric Power Industry, Yokosuka, Kanagawa 240-0196, Japan*
[b]*Graduate School of Energy Science, Kyoto University, Kyoto 606-8501, Japan*
[c]*Japan Science and Technology Agency, ALCA, Chiyoda, Tokyo 102-0076, Japan*

Abstract

$REBa_2Cu_3O_y$ (REBCO; RE: rare-earth elements)-coated conductors (CCs) have high potential for use in superconducting devices. In particular, REBCO CCs are useful for superconducting devices working at relatively high temperatures near 77 K. The important issues in their applications are high performance, reliability and low cost. To date, sufficient performance for some applications has almost been achieved by considerable efforts. The establishment of the reliability of superconducting devices is under way at present. The issue of low cost must be resolved to realize the application of superconducting devices in the near future. Therefore, we have attempted several ways to reduce the cost of REBCO CCs. The coated conductors using a Nb-doped $SrTiO_3$ buffer layer and Ni-plated Cu and stainless steel laminate metal tapes have recently been developed to eliminate the use of electric stabilization layers of Cu and Ag, which are expected to reduce the material cost. Good superconducting properties are obtained at 77 K. The critical current density (J_C) at 77 K under a magnetic self-field is determined to be more than $2x10^6$ A/cm^2. The microstructures of the CCs are analyzed by transmission electron microscopy to obtain a much higher quality. By microscopic structure analysis, an overgrowth of the buffer layer is observed at a grain boundary of the metal substrate, which is one of the reasons for the high J_C.

Peer-review under responsibility of the ISS 2015 Program Committee

Keywords: Coated Conductors;Conductive buffer layers; TEM; Microstrcutures; YBCO

* Corresponding author. Tel.: +81-46-856-2121; fax: +81-46-856-3540.
E-mail address: ai@criepi.denken.or.jp

Peer-review under responsibility of the ISS 2015 Program Committee
doi:10.1016/j.phpro.2016.04.010

1. Introduction

Since the discovery of high-T_C superconductors, the fabrication and improvement of superconducting wires have been conducted by numerous research institutes. Owing to considerable effort, $Bi_2Sr_2Ca_2Cu_3O_{10}$ silver-sheathed wires (Bi2223 SS wires) have already been commercialized [1]. Several superconducting devices, such as superconducting cables [2], motors [3] and generators [4], have been developed. However, the cost of the Bi2223 SS wires is considered to be a limitation because the fabrication of the Bi2223 SS wires uses expensive mass silver. Therefore, $REBa_2Cu_3O_y$ (REBCO, RE: rare-earth element)-coated conductors have been developed as second-generation wires to reduce the wire cost. The coated conductors have recently been commercialized [5-7]; however, they are still expensive. According to our cost analysis of the coated conductors, metal tapes, such as NiW and Hastelloy, and an electric stabilization layer using silver and copper layers are the major causes of the high cost. Consequently, NiW and Hastelloy will be replaced with common metals, such as copper or stainless steel, and metal tapes will be used as an electric stabilization layer by using a conductive buffer layer instead of silver and copper layers. The new and conventional architectures of the coated conductors are described in Fig. 1. This is the first attempt to determine the feasibility of our concept. Therefore, the architecture of the coated conductors became purposely much simpler; it is composed of a biaxially textured metal tape, a Nb-doped $SrTiO_3$ layer as a conductive buffer layer, and a $YBa_2Cu_3O_y$ (YBCO) layer as a superconducting layer.

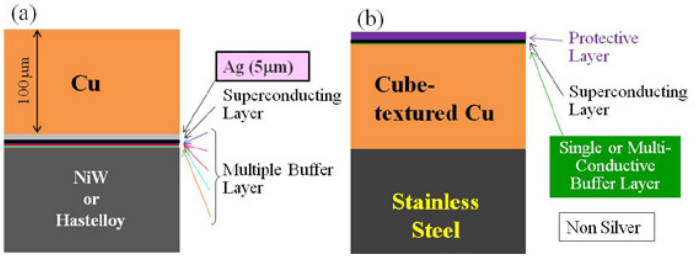

Fig. 1. New and conventional architecture of coated conductors.

In this study, the obtained sample with the new architecture was characterized by X-ray diffraction (XRD) measurements and a critical current density (J_C) measurement at 77 K under a magnetic self-field. Furthermore, because the sample exhibited relatively good properties, the microstructures were examined in detail by transmission electron microscopy (TEM).

2. Experimental Procedure

Metal tapes were obtained from Tanaka Kikinzoku Kogyo Co. Cube-textured Cu and stainless tapes were bonded by a surface activated bonding technique [8]. The Cu surfaces were polished to be clean and smooth by electrolytic polishing. Then, a 500nm Ni layer was fabricated by electroplating, and Nb-doped $SrTiO_3$ (Nb-STO) was selected as a conductive buffer layer, which was deposited by pulsed-laser deposition using a KrF excimer laser. Finally, YBCO layer was deposited by pulsed-laser deposition in the different chamber for the buffer layer fabrication. The nominal composition of the target was $Y_{0.9}Ba_2Cu_3O_y$ owing to the suppression of the yttrium-rich impurity phase. Because YBCO did not properly grow in the upper regions of the yttrium-rich impurity phase, holes were sometimes observed in YBCO layer in the cross-sectional TEM or surface SEM images. Deposition conditions of the buffer and YBCO layers are listed in Table I.

Table I. Preparation conditions of the buffer and YBCO layers

Conditions	Nb-doped $SrTiO_3$	YBCO
Wavelength (nm)	248	248
Frequency (Hz)	20	2
Laser Energy (mJ)	240	200
Gas	2%H_2+98%Ar	O_2
Pressure (Pa)	$1.2x10^{-2}$	35
Temperature (ºC)	600	790
Thickness (nm)	120	160

The structure analysis of the obtained films was carried out by XRD and TEM. J_C was measured at 77 K under a magnetic self-field by a four probe method. XRD θ-2θ scan was measured to determine the phase identity and crystal orientation. The pole figure was measured to confirm the biaxial alignment of the buffer and YBCO layers using the Nb-STO (110) and YBCO (103) peaks. TEM samples were prepared by cutting and milling using a focused-ion beam. Microscopic structure analysis

was conducted by TEM (JEOL JEM-2100F) with energy-dispersive X-ray spectroscopy (EDX).

3. Results and Discussions

A Nb-STO layer and a YBCO layer were observed to only exhibit the (200) and (00ℓ) peaks in XRD θ-2θ scans. Pole figures of Nb-STO (110) and YBCO (103) are shown in Fig. 2. Both pole figures have fourfold symmetry. Therefore, according to XRD θ-2θ scan and pole figure measurements, Nb-STO and YBCO were found to have biaxial alignment. The J_C at 77 K under a magnetic self-field was calculated to be 2.6 MA/cm^2 using a thickness of 160 nm estimated from a scanning TEM image. This value is sufficiently high to indicate that the new architecture has sufficient potential to obtain high-performance coated conductors.

The microstructures of this sample were observed by TEM to evaluate the local crystal orientation and reaction at each interface. Figure 3 shows a cross-sectional scanning TEM (STEM) image with low magnification. A grain boundary can be clearly observed in the cube-textured Cu tape shown in Fig. 3. The structure of the metal surface at the grain boundary became non-flat surface owing to a groove formed by the grain boundary. However, the structure of Nb-STO at the grain boundary was as well as those in the other regions. Furthermore, bright contrast regions were observed at the top of the metal tape. Figure 4 shows a cross-sectional TEM image and local electron diffractions. According to these diffractions, although the neighboring plane spaces of Figs. 4(b) and 4(c) were almost the same, the neighboring plane space in Fig. 4(d) was obviously wider than those in Figs. 4(b) and 4(c). This bright region was concluded to be NiO from both the neighboring plane space and the results of the EDX mapping shown in Fig. 5. The electric diffraction pattern in Fig. 4(f) was the typical pattern of the perovskite structure, indicating a region of Nb-STO. The relationships among Cu, Ni, NiO, Nb-STO and YBCO were Cu(100) // Ni(100) // NiO(100) // Nb-STO(100) // YBCO(001) in perpendicular to the substrate surface. The in-plane crystal orientation of Nb-STO and YBCO was matched with that of the cube-textured Cu tape.

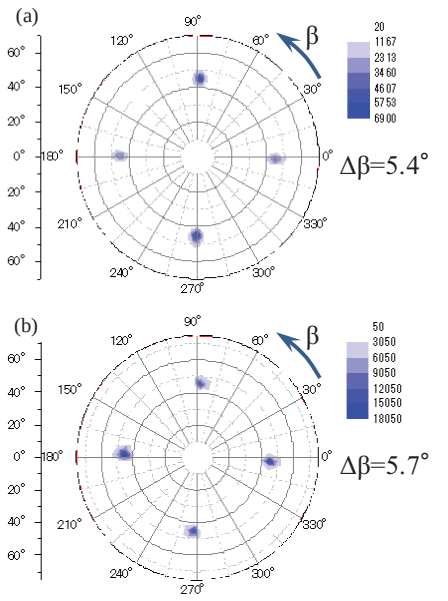

Fig. 2. X-ray pole figures of Nb-STO (110) (a) and YBCO (103) (b). Both figures have fourfold symmetry, indicating that Nb-STO and YBCO have in-plane orientations.

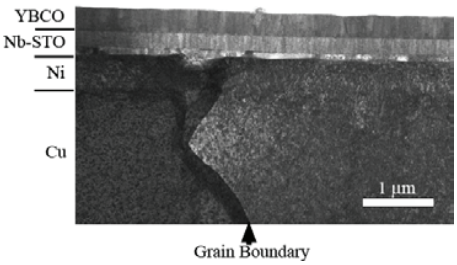

Fig. 3. STEM image of YBCO/Nb-STO/Ni/Cu/stainless steel.

A cross-sectional STEM image near the interface is shown in Fig. 5(d). EDX mapping images corresponding to the STEM image in Fig. 5(d) are shown in Figs. 5(a)-5(c). The interface between Cu and stainless steel laminate tapes is not observed in Fig. 3. The interface between Cu and Ni was observed in Fig.3, but it was unclear and showed a slight contrast change. The interface between Cu and Ni in EDX mapping was also unclear, indicating that Cu and Ni were interdiffused with each other. Therefore, the interface between Cu and Ni could not be distinctly observed in the structural image. Moreover, the Ni did not detect in the YBCO layer in Fig. 5. The Nb-STO buffer layer worked to prevent the Ni diffusion, resulting that the YBCO showed relatively high-J_C. On the other hand, a bright part was observed at the interface between the metal tape and the Nb-STO buffer layer in Figs. 3 and 5. The thickness of the bright layer of the metal tape surface was varied. This layer was found to be nickel oxide according to the EDX mapping results in Figs. 5(a) and 5(b). The interface between the buffer layer and the superconducting layer was very smooth, and an undulation with a period longer than 1 μm that resulted from tape flatness was

observed. Although they were observed in the cross-sectional STEM images, the grooves and oxide layers did not affect the Nb-STO growth. As one possibility, the grooves and oxide layers of the metal tape surface formed during the YBCO deposition, because the YBCO layer was grown at a higher temperature and a higher oxygen pressure than the Nb-STO buffer layer. If this assumption is correct, it can be understood that the grooves and oxide layers do not affect the Nb-STO growth. In this case, the grooves or oxide layers might be considered to cause the peel-off of the Nb-STO buffer layer in actual use or to hinder the passing of current to the substrate when resistance occurred. Therefore, conductive buffer layers that can be used to prevent oxygen diffusion should be developed.

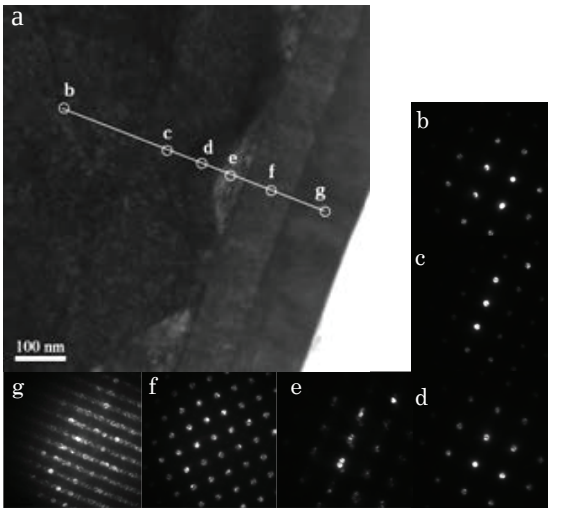

Fig. 4. Cross-sectional TEM image (a) and electron diffraction patterns (b)- (g).

4. Conclusions

The first attempt using the Nb-STO buffer layer was successfully carried out to obtain a high-J_C YBCO layer to eliminate the use of electron stabilization layers. The critical current density at 77 K under a magnetic self-field was 2.6 MA/cm^2. By microstructure analysis, the grooves due to the grain boundaries of metal tapes and the nickel oxide layer due to metal oxidation during YBCO deposition were observed. However, the Nb-STO buffer layer was not affected by the grooves and oxide layers of the metal tape surface. This was considered to be one reason why this superconducting tape had a very high J_C. The present architecture of YBCO/Nb-STO/Ni/Cu/stainless steel might not be the best because the grooves and oxide layers might be problems in practical applications. The new architecture of the coated conductors must be continuously investigated to search for new materials and to optimize fabrication processes to realize real low-cost coated conductors.

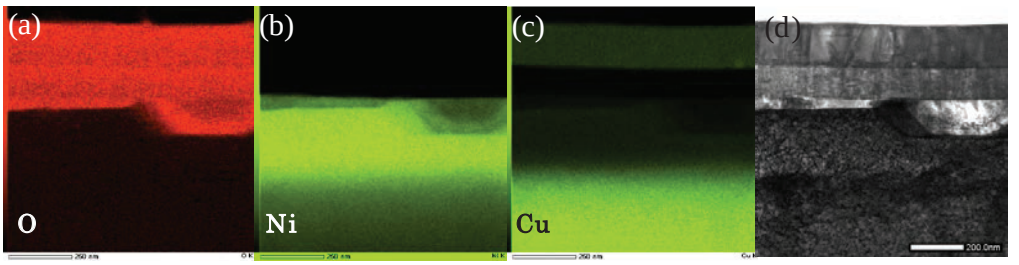

Fig. 5. STEM image and EDX mapping images of O, Ni and Cu elements in the same region.

References

[1] T. Kagiyama, K. Yamazaki, M. Kikuchi, S. Yamade, T. Nakashima, S. Kobayashi, K. Hayashi, K. Sato, J. Shimoyama, M. Inoue, K. Higashikawa, T. Kiss, H. Kitaguchi and H. Kumakura, IOP Conf. Ser.: Mater. Sci. Eng. 18 (2011) 152001.
[2] M. Ohya, Y. Ashibe, M. Watanabe, H. Yumura, Tatsuo, N., H. Hirota, T. Masuda, H. Ichikawa, T. Mimura, S. Honjo and T. Hara, J. Int. Counc. Electr. Eng. 3, issue 2 (2013) 115-120.
[3] T. Nakamura, K. Matsumura, T. Nishimura, K. Nagao, Y. Yamada, N. Amemiya, Y. Itoh, T. Terazawa and K. Osamura, Supercond. Sci. Technol. 24 (2011) 015014.
[4] M. D. Ainslie, A. George, R. Shaw, L. Dawson, A .Winfield, M. Steketee4 and S. Stockley, J. Phys.: Conf. Ser. 507 (2014) 032002.
[5] H. Song, P. Brownsey, Y. Zhang, J. Waterman, T. Fukushima, and D. Hazelton, IEEE Trans. Appl. Supercond. 23 (2013) 4600806.
[6] S. Fleshler, K. DeMoranville, J. Gannon Jr., X. Li, E. Podtburg, M. W. Rupich, S. Sathyamurthy, C. L. H. Thieme, D. Tucker, and L. Whitman, J. Phys.: Conf. Ser. 507 (2014) 02200.
[7] Y. Iijima, Fujikura Tech. Rev. 42 (2013) 117.
[8] N. Kashima, S. Kubota, K. Shima, T. Doi, S. Nagaya, M. Inoue, T. Kiss, Jpn. J. Appl. Phys. 50 (2011) 063101.